Published in final edited form as:
Sci Signal. ; 1(37): ra4. doi:10.1126/scisignal.1160755.

Structural Basis of CXCR4 Sulfotyrosine Recognition by the Chemokine SDF-1/CXCL12

Christopher T. Veldkamp[1], **Christoph Seibert**[2], **Francis C. Peterson**[1], **Norberto B. De la Cruz**[1], **John C. Haugner**[1], **Harihar Basnet**[1], **Thomas P. Sakmar**[2], and **Brian F. Volkman**[1,*]

1*Department of Biochemistry, Medical College of Wisconsin, 8701 Watertown Plank Road, Milwaukee, WI 53226, USA.*

2*Laboratory of Molecular Biology and Biochemistry, Rockefeller University, 1230 York Avenue, New York, NY 10065, USA.*

Abstract

Stem cell homing and breast cancer metastasis are orchestrated by the chemokine SDF-1 and its receptor CXCR4. Here, we report the nuclear magnetic resonance (NMR) structure of a constitutively dimeric SDF-1 in complex with a CXCR4 fragment that contains three sulfotyrosine residues important for a high-affinity ligand-receptor interaction. CXCR4 bridged the SDF-1 dimer interface so that sulfotyrosines $sTyr^{7}$ and $sTyr^{12}$ of CXCR4 occupied positively charged clefts on opposing chemokine subunits. Dimeric SDF-1 induced intracellular Ca^{2+} mobilization but had no chemotactic activity; instead, it prevented native SDF-1-induced chemotaxis, suggesting that it acted as a potent partial agonist. Our work elucidates the structural basis for sulfotyrosine recognition in the chemokine-receptor interaction and suggests a novel strategy for CXCR4-targeted drug development.

Introduction

Chemokines direct homeostatic and proinflammatory immune responses by activating specific guanine nucleotide-binding protein (G protein)-coupled receptors (GPCRs) to induce cell migration along a gradient of increasing concentration of chemokine. The ~50 known chemokines share a conserved tertiary fold and are grouped into four subfamilies (C, CC, CXC, and CX_3C) according to the spacing of conserved cysteines near the N-terminus. Many chemokine signaling pathways are also vital for cell migration in normal development or in abnormal conditions such as tumor metastasis. For example, the CXC chemokine stromal cell derived factor-1 (SDF-1, also known as CXCL12) and its receptor CXCR4 are essential for proper fetal development. *Sdf1*$^{-/-}$ or *Cxcr4*$^{-/-}$ mice die in utero due to defects in hematopoiesis, vascularization of the intestine, cerebellar formation, and heart development (1–3). CXCR4 is also the major coreceptor for T-tropic (X4) strains of human immunodeficiency virus 1 (HIV-1), and SDF-1 inhibits HIV-1 infection (4–7). Additionally, SDF-1 and CXCR4 mediate cancer cell migration and metastasis (8). Treatment with CXCR4-neutralizing antibodies reduces metastatic tumor formation in a mouse model of human breast cancer (8). CXCR4 is found in cells from over 20 types of cancer, which metastasize to tissues that secrete SDF-1, including the bone marrow, lung, liver, and lymph nodes (9).

Peptides derived from the N-terminal domains of chemokine receptors bind specifically to their respective chemokine ligands (10,11). High-affinity binding to SDF-1 requires the

*Corresponding author. E-mail: E-mail: bvolkman@mcw.edu.

extracellular N-terminal domain of CXCR4 (12), which must be posttranslationally modified by sulfation at three tyrosine residues (Tyr^7, Tyr^{12}, and Tyr^{21}) (13,14). Other chemokine receptors, including CCR5, CCR2B and CX_3CR1, are similarly modified at one or more tyrosine residues (15–18). To define the basis for sulfotyrosine recognition in a chemokine-receptor signaling complex, we solved the structures of the extracellular N-terminal domain of CXCR4 in its unmodified, singly sulfated and fully sulfated forms when bound to its ligand SDF-1. Our nuclear magnetic resonance (NMR) studies revealed a symmetric 2:2 complex in which the binding of CXCR4 stabilized dimeric SDF-1 and each receptor sulfotyrosine occupied a unique site on the chemokine. Unexpectedly, the constitutively dimeric SDF-1 protein, which was employed for structural studies, blocked CXCR4-mediated chemotaxis at low nanomolar concentrations. These results provide the first view of sulfotyrosine recognition in a chemokine-receptor complex at atomic resolution and suggest a novel strategy for inhibition of CXCR4 signaling with oligomeric ligands.

Results

Structure of a Constitutively Dimeric SDF-1

We and others have shown that peptides corresponding to the N-terminus of CXCR4 bind to SDF-1 with micromolar affinity (13,19), but attempts to solve the NMR structure of a complex containing SDF-1 and the N-terminus of CXCR4 were compromised by spectral broadening arising from the equilibrium between monomeric and dimeric forms of SDF-1. Because CXCR4 has been purified as a ligand-independent dimer (20) and binding of the N-terminal 38 residues of CXCR4 (p38) promotes SDF-1 dimerization (13), we engineered an SDF-1 protein to limit exchange between complexes of different stoichiometries. Guided by the crystal structure of SDF-1 (21), we identified Leu^{36} and Ala^{65} as residues at the dimer interface that could be replaced with Cys residues to form a pair of symmetric, intermolecular disulfide bonds (Fig. 1A). The SDF-1 double mutant [SDF1(L36C/A65C)] migrated as a stable dimer under nonreducing SDS-PAGE (Fig. 1B), and its translational self-diffusion coefficient, as measured by pulsed-field gradient NMR, was consistent with that of a dimeric species (22) (Fig. 1C). We confirmed the presence of disulfide bonds linking the two monomers and solved the structure of SDF1(L36C/A65C) by NMR. The structure of covalently-locked, symmetric SDF1 (L36C/A65C) dimer (hereafter referred to as $SDF1_2$) was superimposable on that of a dimer of wild-type SDF-1, which was determined crystallographically (Fig. 1D). $SDF1_2$ displays the canonical chemokine fold in which a flexible N-terminus is connected by the N-loop to a three-stranded antiparallel β-sheet and a C-terminal α-helix.

Chemical Shift Mapping of the p38:$SDF1_2$ Interface

Binding of p38 to ^{15}N-labeled wild-type SDF-1 induced chemical shift perturbations attributable to a combination of SDF-1 dimer formation and peptide binding (13). Gozansky *et al*. observed similar chemical shift patterns following the interaction of SDF-1 with the N-terminus of CXCR4, but incorrectly assumed that SDF-1 was purely monomeric (13,19,23). Hence, the CXCR4 N-terminal binding surface they identified incorrectly included the SDF-1 dimer interface (13,19). Importantly, neither they nor we could solve a structure of native SDF-1 in complex with the N-terminus of CXCR4. Our titration of [U-^{15}N]-p38 with SDF-1, which showed extreme NMR line broadening, explains why no structure could be obtained. The line-broadening resulted from p38 binding to SDF-1 that was fluctuating between its monomeric and dimeric states, thereby producing a weak NMR signal for the CXCR4 peptide and thwarting any chance of determining an NMR structure (13).

Because the locked dimer reduces the number of accessible states, interpretation of NMR spectra of $SDF1_2$ upon its binding to p38 was straightforward. Titration of ^{15}N-labeled $SDF1_2$ with p38 (Fig. 2A) perturbed NMR signals of the residues of the N-loop but not those

of the dimer interface (Fig. 2B), thus isolating signals for likely CXCR4:SDF-1 binding determinants. Because only one set of $SDF1_2$ signals was observed during the p38 titration and because addition of more than two molar equivalents of p38 induced no further chemical shift perturbations, we concluded that a 2:2 complex was formed by the binding of two p38 molecules to symmetric sites on the surface of $SDF1_2$ (Fig. 2C).

Structures of $SDF1_2$:p38 Complexes

Tyrosine sulfation in the N-terminal domain of CXCR4 contributes substantially to the binding of SDF-1 (14). We showed previously that sulfation of Tyr^{21} enhances the affinity of p38 for SDF-1 by ~3-fold (13), and we observed that fully-sulfated p38-sY3 binds ~20-fold more tightly than the unsulfated peptide (apparent $Kd = 0.2 \pm 0.2\ \mu M$; data not shown). To understand the role of sulfotyrosines in CXCR4:SDF-1 binding, we solved the structures of unsulfated, selectively sulfated, and fully sulfated CXCR4 p38 peptides bound to $SDF1_2$. Recombinant [U-^{15}N,13C]-labeled p38 was modified using purified tyrosyl protein sulfotransferase (13) to contain sulfotyrosine at position 21 (p38-sY_1) or positions 7, 12, and 21 (p38-sY_3) (Fig. 3A). Like the p38 and p38-sY_1 peptides (13), free p38-sY_3 displayed no secondary or tertiary structure in solution, and sulfation induced only local chemical shift changes.

For the structure of each complex, NOEs between $SDF1_2$ and the (sulfo)tyrosine side chains of CXCR4 (Fig. 3B) unambiguously defined the location of two p38 molecules on the chemokine. Each p38 peptide bound the chemokine in the same mode irrespective of the extent of sulfation (Fig. 3C–E). Two p38 molecules wrapped around the symmetric $SDF1_2$ dimer in an extended conformation that contained no secondary structure. Specific side chain–mediated contacts defined a path for the bound CXCR4 peptide that corresponded closely to the surface identified by $^1H/^{15}N$ chemical shift perturbations (Fig. 4A). In contrast, residues of the flexible N-terminus and the C-terminal α-helix of $SDF1_2$ were unperturbed by p38 binding, and the overall chemokine structure was unaffected.

CXCR4 stabilized SDF-1 by interacting with both subunits and recognizing unique features of the dimer interface. Near the CXCR4 N-terminus, each p38 peptide crossed the dimer interface such that $sTyr^7$ and $sTyr^{12}$ interacted with opposing SDF-1 subunits (Fig. 4A). In the membrane-proximal portion of the N-terminal domain of CXCR4, NOEs connected Pro^{27} to Gln^{59} in one subunit of $SDF1_2$ and to Leu^{66} in the opposing subunit, where the two C-terminal helices packed against each other. Structures of other sulfotyrosine-containing protein complexes show that the O-sulfonate group typically interacts with a positively charged side chain (24,25). In a similar manner, each negatively-charged sulfotyrosine in CXCR4 occupied a unique positively-charged pocket on the $SDF1_2$ surface (Fig. 4B–D).

NOE constraints from Val^{23} in one subunit of $SDF1_2$ positioned the $sTyr^7$ O-sulfonate to form a favorable electrostatic interaction with a positively-charged Arg^{20} side chain of SDF-1 (Fig. 4B). In a similar fashion, NOEs connected $sTyr^{12}$ of p38 to Pro^{10} and Leu^{29} of the other subunit of $SDF1_2$ and placed the sulfotyrosine within ~3 Å of the positively-charged amino group of Lys^{27} (Fig. 4C). Residues connecting the N-terminal CXC motif with the β1 strand of SDF-1 (the "N loop"), particularly the RFFESH motif consisting of residues 12–17, were predicted from mutagenic studies to interact with the N-terminus of CXCR4 (12,26,27). We observed intermolecular NOEs between $^1H^N$ of Phe^{14} in $SDF1_2$ and the $^1H^\alpha$ of Gly^{19} from CXCR4 and from Val^{18} in the chemokine to $sTyr^{21}$ of p38(Fig. 3B). NOEs also linked $sTyr^{21}$ of p38 with Val^{49} in the β3 strand of $SDF1_2$ and positioned the $sTyr^{21}$ O-sulfonate <5 Å from the guanidinium of Arg^{47} (Fig 4D), consistent with our earlier measurement of sulfotyrosine-specific chemical shift perturbations (13). Chemokine recognition of a receptor sulfotyrosine corresponding to $sTyr^{21}$ by a basic pocket formed between the N-loop and the 40's loop may be a common feature of the CXC family. Residues lining the $sTyr^{21}$-binding pocket of SDF-1 (Val^{18}, Arg^{47}, and Val^{49}) are conserved in at least half of the 16 CXC chemokines (28). A

tyrosine corresponding to sulfotyrosine 21 of CXCR4 may likewise be found in all CXC family receptors except CXCR6. In contrast, neither $sTyr^7$, $sTyr^{12}$ nor their corresponding binding sites are conserved in the CXC receptors or chemokines.

Functional Validation of the SDF1:p38 Interface

To assess the relative contribution of each sulfotyrosine to SDF-1:CXCR4 binding, we designed a series of mutations of native SDF-1 to disrupt the putative binding sites individually and then measured Ca^{2+} mobilization in THP-1 cells, which express CXCR4 (29). We assessed the likely interaction between monomeric SDF-1 and the N-terminus of CXCR4 by looking at half of the $SDF1_2$:p38-sY_3 structure (one SDF-1 subunit and one p38-sY_3). Overall, substitutions in native SDF-1 that altered interactions observed in this model complex (Fig. 5A and B, red) resulted in higher EC_{50} values for CXCR4 activation as measured in Ca^{2+} mobilization assays, whereas substitutions that were not at the binding interface resulted in no change in EC_{50} (Fig. 5A and B, cyan). Table 1 lists the amino acid substitutions and Ca^{2+} mobilization EC_{50} values.

In the $SDF1_2$:p38-sY_3 structure, the $sTyr^7$ O-sulfonate formed a favorable electrostatic interaction with the positively-charged Arg^{20} in the chemokine. However, $sTyr^7$ bound to one SDF-1 subunit whereas the majority of the rest of p38-sY_3 bound to the other SDF-1 subunit. In the model of monomeric SDF-1 and CXCR4 peptide, the site of $sTyr^7$ binding is not identified. It is clear that $sTyr^7$ could not bind to Arg^{20} of monomeric SDF-1, and replacement of Arg^{20} with Ala in native SDF-1 produced no change in EC_{50} (Table 1). This suggests that if $sTyr^7$ forms interactions with monomeric SDF-1, they are not through Arg^{20}. At present, our structural studies cannot identify the location of $sTyr^7$ binding to monomeric SDF-1, if such an interaction occurs.

In both the $SDF1_2$:p38-sY_3 structure and the model, $sTyr^{12}$ of p38-sY_3 bound near to Lys^{27} of $SDF\text{-}1_2$. Substitutions of Ala and Glu acid at this position in SDF-1 increased the EC_{50} for Ca^{2+} mobilization to 10.1 and 16.8 nM, respectively. Val^{39} in the β2 strand of SDF-1 is directly across from Lys^{27} of the β1 strand and a $Val^{39} \rightarrow Ala^{39}$ substitution increased the EC_{50} to 27.1 nM. Also, the $sTyr^{21}$ O-sulfonate is near the guanidinium of Arg^{47} (Fig 4D). An $Arg^{47} \rightarrow Ala^{47}$ substitution in native SDF-1 changed the EC_{50} to 14.1 nM, and replacement of the positively-charged Arg side chain with a negatively-charged Glu drastically altered activation ($Arg^{47} \rightarrow Glu^{47}$, EC_{50} = 654 nM) relative to wild-type SDF-1 (EC_{50} = 3.6 nM). Substitution of Val^{49}, which has NOEs to $sTyr^{21}$, with Ala also showed a 2.4-fold increase in EC_{50}.

In human embryonic kidney (HEK) 293 cells, Tyr^{21} is sulfated to a higher degree than are Tyr^7 and Tyr^{12} and $sTyr^{21}$ contributes the most to SDF-1 binding to the expressed CXCR4 (14). The extent of sulfation of the Tyr residues of CXCR4 has not been characterized in THP-1 cells, but our results are consistent with those of Farzan *et al*. (14) because disruption of the SDF-1 binding site for $sTyr^{21}$ had the greatest effect. The results from our mutagenesis studies are consistent with previous studies and suggest that the structure of $SDF1_2$ with the various CXCR4 peptides contributes to an understanding of the binding and activation of CXCR4 by native SDF-1.

Partial Agonism of CXCR4 by $SDF1_2$

Solving the NMR structure of the $SDF1_2$:CXCR4 complex required that the chemokine exist as a disulfide-stabilized dimer. To determine whether the constitutively dimeric chemokine retained biological activity, we compared Ca^{2+} mobilization and chemotactic responses induced by SDF-1 in THP-1 cells with those of $SDF1_2$. Robust activation of CXCR4 was observed for both wild-type SDF-1 (EC_{50} = 3.6 nM) and $SDF1_2$ (EC_{50} = 12.9 nM) in the Ca^{2+} mobilization assay (Fig. 6A). AMD3100, a small-molecule antagonist of CXCR4 (30),

competed with both ligands with IC_{50} values of 3.3 nM for SDF-1 and 3.2 nM for $SDF1_2$ (data not shown). Unexpectedly, although 1 to 30 nM of wild-type SDF-1 induced chemotactic migration, the constitutively dimeric $SDF1_2$ failed to attract cells in a transwell chemotaxis assay at concentrations of up to 1 μM (Fig. 6B). Because $SDF1_2$ bound to CXCR4 and induced a Ca^{2+} mobilization response but exhibited no chemotactic activity, we speculated that it might block chemotaxis in response to wild-type SDF-1. Indeed, migration of THP-1 cells in response to 10 nM wild-type SDF-1 was potently inhibited by increasing concentrations of $SDF1_2$ (IC_{50} = 4 nM) (Fig. 6C).

Alterations in Chemotactic Signaling Through Changes in the Ratio of SDF-1 Monomers to Dimers

In cell-based assays, chemokines typically induce chemotactic migration over a relatively narrow concentration range. Like other chemokines, SDF-1 exhibited a biphasic concentration dependence that decreased and ultimately ceased at higher concentrations (Fig. 6B). Because the locked $SDF1_2$ dimer inhibited chemotaxis (Fig. 6C), we speculated that low concentrations of monomeric SDF-1 might stimulate chemotaxis, whereas dimeric SDF-1, promoted by binding to heparin or CXCR4, might be present at higher concentrations and could therefore interfere with chemotactic signaling.

To test this hypothesis, we conducted chemotaxis assays in which we compared the responses of cells to an SDF-1 mutant that remains monomeric at higher concentrations to the responses of cells to wild-type SDF-1. If inactivation is indeed due to dimerization, SDF1(H25R), which has a dimer Kd ~10-fold higher than SDF-1 (22), should resist inactivation at higher concentrations and maintain a chemotactic response at concentrations at which the activity of SDF-1 decreases. Both proteins induced a dose-dependent chemotactic response from 1–30 nM and had similar EC50 values in Ca^{2+} mobilization assays, but SDF1(H25R) promoted cell migration much more strongly than did SDF-1 at higher concentrations (70–100 nM) before returning to baseline levels (Fig. 6D). Based on these results, we speculate that a shift in the oligomeric state of SDF-1 regulates chemotaxis, perhaps through a change in the kinetics of CXCR4 internalization.

Discussion

Tyrosine sulfation has been predicted or observed for the N-terminal extracellular domain of most chemokine receptors (31). This post-translational modification contributes to high affinity binding of chemokine ligands and other binding partners such as the gp120 protein of HIV-1 (15). The structures of the SDF-1:CXCR4 complexes reported here provide the first illustration of how chemokines can recognize specific patterns of sulfotyrosine modification in their respective receptors. We validated these structural results in the context of the wild-type chemokine by performing functional assays on a panel of SDF-1 mutant proteins. Substitution of residues that interact with CXCR4 in the $SDF1_2$:p38-sY_3 complex correlates strongly with changes in the EC_{50} for Ca^{2+} mobilization response in THP-1 cells. We previously reported that binding to the N-terminus of CXCR4 promotes SDF-1 dimer formation (13). It is now clear that the N-terminus of CXCR4 promotes dimerization of SDF-1 by contacting specific sulfotyrosine recognition sites on both sides of the dimer interface.

Although the functional role of chemokine dimers is not fully understood (32–37), dimerization is essential for the in vivo function of the CC chemokines monocyte chemoattractant protein 1 (MCP-1), RANTES [regulated upon activation, normal T cell-expressed and –secreted], and macrophage inflammatory protein 1β (MIP-1β) (38) and the CXC chemokine interferon-induced protein of 10 kD (IP-10, also known as CXCL10) (39). Structural differences between CC dimers and CXC dimers result in markedly different capacities for binding to GPCRs. The N-terminus of a CC chemokine participates directly in receptor activation (40), but also forms

the dimer interface. Consequently, a disulfide-linked MIP-1β dimer fails to bind to its receptor CCR5 because critical binding determinants are buried in the dimer interface (37). In contrast, the N-terminus in a CXC chemokine dimer remains available for receptor interactions (41). A disulfide-linked dimeric form of the CXC chemokine interleukin-8 (IL-8) induces a Ca^{2+} mobilization response in neutrophils with an EC_{50} (1.5 nM) comparable to that of wild-type IL-8 (4.5 nM) (32). Thus, whereas CC chemokines seem to act on their receptors exclusively as monomers, monomers and dimers may both participate in CXC chemokine signaling. Other physiological binding partners, such as heparin, can promote chemokine dimer formation, as we showed for SDF-1 (22). Also, in the solved structure of SDF-1 with a heparin disaccharide, SDF-1 is present as a dimer (42). Because residues such as Lys^{27} of SDF-1 are involved in binding to both heparin and CXCR4, one function of the N-terminus of CXCR4 may be to displace heparin prior to receptor binding.

If SDF-1 dimer formation alters CXCR4 signaling, as our results indicate (Fig. 6B and 6D), is there also a role for CXCR4 receptor dimerization? Chemokine receptors and other GPCRs are widely proposed to exist and function as dimers (43–46), but their detection and characterization remain controversial (47, 48). Our results do not report directly on the oligomeric state of the receptor, but CXCR4 has been purified from cells as a homodimer (20) and the structure of $SDF1_2$:p38 (Fig. 4A) illustrates how binding to the CXCR4 N-terminus promotes the dimerization of SDF-1 (13). Residues in the flexible N-terminus of SDF-1 are responsible for CXCR4 activation and thus may correspond to small molecule agonists of other GPCRs, such as for the β_2-adrenergic receptor (β_2-AR) (26, 49). The spacing of the ligand-binding sites in the crystal structure of dimeric β_2-AR (50, 51) matches the ~40 Å distance separating the N-termini of an SDF-1 dimer, which suggests that formation of a functional 2:2 SDF-1:CXCR4 complex might be plausible. To account for the observed inhibition of CXCR4-mediated chemotaxis by $SDF1_2$ (Fig. 6C), we propose a model in which monomeric SDF-1 activates the full complement of signaling pathways required for chemotaxis, but binding of the dimeric ligand produces a 2:2 chemokine:receptor complex that stimulates intracellular calcium signaling but prevents cell migration (Fig. 6E).

Our results reveal the first details of sulfotyrosine recognition by a chemokine, and provide a structural basis for the enhancement of chemokine binding affinity by this posttranslational modification. In addition, the structures of $SDF1_2$ explain why binding to the N-terminus of CXCR4 induces dimerization of SDF-1 (13). However, the $SDF1_2$:p38 structure also illustrates an unexpected mode of chemokine inhibition. As a full agonist, wild-type SDF-1 induces a Ca^{2+} mobilization response and chemotactic migration. In measurements of THP-1 cells, $SDF1_2$ is both a partial CXCR4 agonist, stimulating Ca^{2+} mobilization, and a selective antagonist that blocks chemotaxis. Additional experiments are required to demonstrate whether inhibition by ligand dimerization is a general feature of the CXC chemokine family, which could be exploited for therapeutic benefit.

Materials and Methods

Structure Determination

Tyrosine sulfation of CXCR4 p38 peptides was performed as described elsewhere (13). Two samples were used for each structure determination: [U-^{15}N,^{13}C]-$SDF1_2$ with unlabeled p38 peptide, and [U-^{15}N,^{13}C]-p38 with unlabeled $SDF1_2$ using a 1:1.25 (monomer subunit) molar ratio of labeled to unlabeled components in each case. Standard NMR techniques were used for generating chemical shift assignments for ^{15}N/^{13}C-labeled $SDF1_2$, p38, sY_1 p38 and sY_1 p38 (52). 3-dimensional ^{15}N-edited NOESY-HSQC, ^{13}C-edited NOESY-HSQC, and ^{13}C (aromatic)-edited NOESY-HSQC spectra (τ_{mix} = 80 ms) were used to generate distance constraints. Intermolecular distance constraints were obtained from a 3D F1-^{13}C-filtered/F3-^{13}C-edited NOESY-HSQC spectrum (τ_{mix} = 120 ms). Backbone dihedral angle constraints

were obtained from $^{1}H^{\alpha}$, $^{13}C^{\alpha}$, $^{13}C^{\beta}$, $^{13}C'$, and ^{15}N secondary shifts using TALOS. Initial structures were calculated using the NOEASSIGN module of the torsion angle dynamics program CYANA followed by iterative manual refinement to eliminate constraint violations. X-PLOR was used for further refinement, in which physical force field terms and explicit water solvent molecules were added to the experimental constraints. Tables S1 to S4 list the statistics for Procheck-NMR validation of the final 20 conformers.

Functional Assays

THP-1 cells, a monocytic leukemia cell line, were obtained from ATCC. Ca^{2+}-dependent Fluo-3 emission was measured at 25°C using a PTI spectrofluorometer with an excitation wavelength of 505 nm and emission was detected at 525 nm. Immediately before measurement, an aliquot of cells was washed and resuspended and allowed to equilibrate at 25°C for five minutes in the cuvette. After establishing a baseline (~100 s), chemokine was added and the Ca^{2+} mobilization response was monitored for ~350 seconds. Total fluorescence intensity was measured after lysing cells with 1% Triton X-100, followed by the addition of 50 mM EDTA. Ca^{2+} mobilization signals are reported as the ratio of the chemokine-induced fluorescence intensity maximum and the fluorescence intensity after cell lysis. Chemotaxis was assayed using Transwells (5 μm pore; Costar, Cambridge, MA). THP-1 cells were washed with PBS and migration buffer (RPMI 1640 containing 2 mg/mL of bovine serum albumin). 5×10^5 cells in 100 μL were placed in the top well and migration buffer containing the indicated doses of chemokine was added to the bottom wells. Plates were incubated for 3 h at 37°C and 5% CO_2. Transwell inserts were then removed and cells that had migrated into the lower chamber were counted using a hematocytometer. Assays were also performed with SDF-1 present in both the lower and upper chambers or with no SDF-1 in the lower chamber as controls to measure chemokinesis and basal migration, respectively. The chemotactic index is computed as the number of cells that migrated in response to chemokine divided by the number of cells counted in the absence of chemokine.

Supplementary Material

Refer to Web version on PubMed Central for supplementary material.

References

1. Nagasawa T, Hirota S, Tachibana K, Takakura N, Nishikawa S, Kitamura Y, Yoshida N, Kikutani H, Kishimoto T. Defects of B-cell lymphopoiesis and bone-marrow myelopoiesis in mice lacking the CXC chemokine PBSF/SDF-1. Nature 1996;382:635. [PubMed: 8757135]
2. Tachibana K, Hirota S, Iizasa H, Yoshida H, Kawabata K, Kataoka Y, Kitamura Y, Matsushima K, Yoshida N, Nishikawa S, Kishimoto T, Nagasawa T. The chemokine receptor CXCR4 is essential for vascularization of the gastrointestinal tract. Nature 1998;393:591. [PubMed: 9634237]
3. Zou YR, Kottmann AH, Kuroda M, Taniuchi I, Littman DR. Function of the chemokine receptor CXCR4 in haematopoiesis and in cerebellar development. Nature 1998;393:595. [PubMed: 9634238]
4. Bleul CC, Farzan M, Choe H, Parolin C, Clark-Lewis I, Sodroski J, Springer TA. The lymphocyte chemoattractant SDF-1 is a ligand for LESTR/fusin and blocks HIV-1 entry. Nature 1996;382:829. [PubMed: 8752280]
5. Feng Y, Broder CC, Kennedy PE, Berger EA. HIV-1 entry cofactor: functional cDNA cloning of a seven-transmembrane, G protein-coupled receptor. Science 1996;272:872. [PubMed: 8629022]
6. D′Souza MP, Harden VA. Chemokines and HIV-1 second receptors. Confluence of two fields generates optimism in AIDS research. Nature medicine 1996;2:1293.
7. D′Souza MP, Cairns JS, Plaeger SF. Current evidence and future directions for targeting HIV entry: therapeutic and prophylactic strategies. Jama 2000;284:215. [PubMed: 10889596]

8. Muller A, Homey B, Soto H, Ge N, Catron D, Buchanan ME, McClanahan T, Murphy E, Yuan W, Wagner SN, Barrera JL, Mohar A, Verastegui E, Zlotnik A. Involvement of chemokine receptors in breast cancer metastasis. Nature 2001;410:50. [PubMed: 11242036]
9. Zlotnik A. Chemokines and cancer. Int J Cancer 2006;119:2026. [PubMed: 16671092]
10. Gayle RB 3rd, Sleath PR, Srinivason S, Birks CW, Weerawarna KS, Cerretti DP, Kozlosky CJ, Nelson N, Vanden Bos T, Beckmann MP. Importance of the amino terminus of the interleukin-8 receptor in ligand interactions. The Journal of biological chemistry 1993;268:7283. [PubMed: 8463264]
11. Mizoue LS, Bazan JF, Johnson EC, Handel TM. Solution structure and dynamics of the CX3C chemokine domain of fractalkine and its interaction with an N-terminal fragment of CX3CR1. Biochemistry 1999;38:1402. [PubMed: 9931005]
12. Doranz BJ, Orsini MJ, Turner JD, Hoffman TL, Berson JF, Hoxie JA, Peiper SC, Brass LF, Doms RW. Identification of CXCR4 domains that support coreceptor and chemokine receptor functions. J Virol 1999;73:2752. [PubMed: 10074122]
13. Veldkamp CT, Seibert C, Peterson FC, Sakmar TP, Volkman BF. Recognition of a CXCR4 sulfotyrosine by the chemokine stromal cell-derived factor-1alpha (SDF-1alpha/CXCL12). J Mol Biol 2006;359:1400. [PubMed: 16725153]
14. Farzan M, Babcock GJ, Vasilieva N, Wright PL, Kiprilov E, Mirzabekov T, Choe H. The role of post-translational modifications of the CXCR4 amino terminus in stromal-derived factor 1 alpha association and HIV-1 entry. The Journal of biological chemistry 2002;277:29484. [PubMed: 12034737]
15. Farzan M, Mirzabekov T, Kolchinsky P, Wyatt R, Cayabyab M, Gerard NP, Gerard C, Sodroski J, Choe H. Tyrosine sulfation of the amino terminus of CCR5 facilitates HIV-1 entry. Cell 1999;96:667. [PubMed: 10089882]
16. Farzan M, Chung S, Li W, Vasilieva N, Wright PL, Schnitzler CE, Marchione RJ, Gerard C, Gerard NP, Sodroski J, Choe H. Tyrosine-sulfated peptides functionally reconstitute a CCR5 variant lacking a critical amino-terminal region. The Journal of biological chemistry 2002;277:40397. [PubMed: 12183462]
17. Seibert C, Cadene M, Sanfiz A, Chait BT, Sakmar TP. Tyrosine sulfation of CCR5 N-terminal peptide by tyrosylprotein sulfotransferases 1 and 2 follows a discrete pattern and temporal sequence. Proc Natl Acad Sci U S A 2002;99:11031. [PubMed: 12169668]
18. Fong AM, Alam SM, Imai T, Haribabu B, Patel DD. CX3CR1 tyrosine sulfation enhances fractalkine-induced cell adhesion. The Journal of biological chemistry 2002;277:19418. [PubMed: 11909868]
19. Gozansky EK, Louis JM, Caffrey M, Clore GM. Mapping the binding of the N-terminal extracellular tail of the CXCR4 receptor to stromal cell-derived factor-1alpha. J Mol Biol 2005;345:651. [PubMed: 15588815]
20. Babcock GJ, Farzan M, Sodroski J. Ligand-independent dimerization of CXCR4, a principal HIV-1 coreceptor. The Journal of biological chemistry 2003;278:3378. [PubMed: 12433920]
21. Ohnishi Y, Senda T, Nandhagopal N, Sugimoto K, Shioda T, Nagal Y, Mitsui Y. Crystal structure of recombinant native SDF-1alpha with additional mutagenesis studies: an attempt at a more comprehensive interpretation of accumulated structure-activity relationship data. J Interferon Cytokine Res 2000;20:691. [PubMed: 10954912]
22. Veldkamp CT, Peterson FC, Pelzek AJ, Volkman BF. The monomer-dimer equilibrium of stromal cell-derived factor-1 (CXCL 12) is altered by pH, phosphate, sulfate, and heparin. Protein Sci 2005;14:1071. [PubMed: 15741341]
23. Baryshnikova OK, Sykes BD. Backbone dynamics of SDF-1alpha determined by NMR: interpretation in the presence of monomer-dimer equilibrium. Protein Sci 2006;15:2568. [PubMed: 17075134]
24. Vijayalakshmi J, Padmanabhan KP, Mann KG, Tulinsky A. The isomorphous structures of prethrombin2, hirugen-, and PPACK-thrombin: changes accompanying activation and exosite binding to thrombin. Protein Sci 1994;3:2254. [PubMed: 7756983]
25. Somers WS, Tang J, Shaw GD, Camphausen RT. Insights into the molecular basis of leukocyte tethering and rolling revealed by structures of P- and E-selectin bound to SLe(X) and PSGL-1. Cell 2000;103:467. [PubMed: 11081633]
26. Crump MP, Gong JH, Loetscher P, Rajarathnam K, Amara A, Arenzana-Seisdedos F, Virelizier JL, Baggiolini M, Sykes BD, Clark-Lewis I. Solution structure and basis for functional activity of stromal

cell- derived factor-1; dissociation of CXCR4 activation from binding and inhibition of HIV-1. Embo J 1997;16:6996. [PubMed: 9384579]

27. Heveker N, Montes M, Germeroth L, Amara A, Trautmann A, Alizon M, Schneider-Mergener J. Dissociation of the signalling and antiviral properties of SDF-1- derived small peptides. Curr Biol 1998;8:369. [PubMed: 9545196]
28. Peterson FC, Thorpe JA, Harder AG, Volkman BF, Schwarze SR. Structural determinants involved in the regulation of CXCL14/BRAK expression by the 26 S proteasome. J Mol Biol 2006;363:813. [PubMed: 16987528]
29. Princen K, Hatse S, Vermeire K, De Clercq E, Schols D. Evaluation of SDF-1/CXCR4-induced Ca^{2+} signaling by fluorometric imaging plate reader (FLIPR) and flow cytometry. Cytometry 2003;51A:35. [PubMed: 12500303]
30. Donzella GA, Schols D, Lin SW, Este JA, Nagashima KA, Maddon PJ, Allaway GP, Sakmar TP, Henson G, De Clercq E, Moore JP. AMD3100, a small molecule inhibitor of HIV-1 entry via the CXCR4 co-receptor. Nature medicine 1998;4:72.
31. Liu J, Louie S, Hsu W, Yu KM, Nicholas HB Jr, Rosenquist GL. Tyrosine Sulfation Is Prevalent in Human Chemokine Receptors Important in Lung Disease. Am J Respir Cell Mol Biol. 2008
32. Williams G, Borkakoti N, Bottomley GA, Cowan I, Fallowfield AG, Jones PS, Kirtland SJ, Price GJ, Price L. Mutagenesis studies of interleukin-8. Identification of a second epitope involved in receptor binding. The Journal of biological chemistry 1996;271:9579. [PubMed: 8621632]
33. Leong SR, Lowman HB, Liu J, Shire S, Deforge LE, Gillece-Castro BL, McDowell R, Hebert CA. IL-8 single-chain homodimers and heterodimers: interactions with chemokine receptors CXCR1, CXCR2, and DARC. Protein Sci 1997;6:609. [PubMed: 9070443]
34. Fernando H, Chin C, Rosgen J, Rajarathnam K. Dimer dissociation is essential for interleukin-8 (IL-8) binding to CXCR1 receptor. The Journal of biological chemistry 2004;279:36175. [PubMed: 15252057]
35. Rajarathnam K, Prado GN, Fernando H, Clark-Lewis I, Navarro J. Probing receptor binding activity of interleukin-8 dimer using a disulfide trap. Biochemistry 2006;45:7882. [PubMed: 16784240]
36. Schnitzel W, Monschein U, Besemer J. Monomer-dimer equilibria of interleukin-8 and neutrophil-activating peptide 2. Evidence for IL-8 binding as a dimer and oligomer to IL-8 receptor B. J Leukoc Biol 1994;55:763. [PubMed: 8195702]
37. Jin H, Shen X, Baggett BR, Kong X, Liwang PJ. The human CC chemokine MIP-1beta dimer is not competent to bind to the CCR5 receptor. The Journal of biological chemistry. 2007
38. Proudfoot AE, Handel TM, Johnson Z, Lau EK, LiWang P, Clark-Lewis I, Borlat F, Wells TN, Kosco-Vilbois MH. Glycosaminoglycan binding and oligomerization are essential for the in vivo activity of certain chemokines. Proc Natl Acad Sci U S A 2003;100:1885. [PubMed: 12571364]
39. Campanella GS, Grimm J, Manice LA, Colvin RA, Medoff BD, Wojtkiewicz GR, Weissleder R, Luster AD. Oligomerization of CXCL10 is necessary for endothelial cell presentation and in vivo activity. J Immunol 2006;177:6991. [PubMed: 17082614]
40. Baggiolini M, Dewald B, Moser B. Human chemokines: an update. Annu Rev Immunol 1997;15:675. [PubMed: 9143704]
41. Clore GM, Gronenborn AM. Three-dimensional structures of alpha and beta chemokines. Faseb J 1995;9:57. [PubMed: 7821760]
42. Murphy JW, Cho Y, Sachpatzidis A, Fan C, Hodsdon ME, Lolis E. Structural and functional basis of CXCL12 (stromal cell-derived factor-1 alpha) binding to heparin. The Journal of biological chemistry 2007;282:10018. [PubMed: 17264079]
43. Milligan G, Smith NJ. Allosteric modulation of heterodimeric G-protein-coupled receptors. Trends Pharmacol Sci 2007;28:615. [PubMed: 18022255]
44. El-Asmar L, Springael JY, Ballet S, Andrieu EU, Vassart G, Parmentier M. Evidence for negative binding cooperativity within CCR5-CCR2b heterodimers. Mol Pharmacol 2005;67:460. [PubMed: 15509716]
45. Springael JY, Urizar E, Parmentier M. Dimerization of chemokine receptors and its functional consequences. Cytokine Growth Factor Rev 2005;16:611. [PubMed: 15979374]
46. Bouvier M, Heveker N, Jockers R, Marullo S, Milligan G. BRET analysis of GPCR oligomerization: newer does not mean better. Nat Methods 2007;4:3. [PubMed: 17195017]

47. James JR, Oliveira MI, Carmo AM, Iaboni A, Davis SJ. A rigorous experimental framework for detecting protein oligomerization using bioluminescence resonance energy transfer. Nat Methods 2006;3:1001. [PubMed: 17086179]

48. Chabre M, le Maire M. Monomeric G-protein-coupled receptor as a functional unit. Biochemistry 2005;44:9395. [PubMed: 15996094]

49. Loetscher P, Gong JH, Dewald B, Baggiolini M, Clark-Lewis I. N-terminal peptides of stromal cell-derived factor-1 with CXC chemokine receptor 4 agonist and antagonist activities. The Journal of biological chemistry 1998;273:22279. [PubMed: 9712844]

50. Rosenbaum DM, Cherezov V, Hanson MA, Rasmussen SG, Thian FS, Kobilka TS, Choi HJ, Yao XJ, Weis WI, Stevens RC, Kobilka BK. GPCR engineering yields high-resolution structural insights into beta2-adrenergic receptor function. Science 2007;318:1266. [PubMed: 17962519]

51. Cherezov V, Rosenbaum DM, Hanson MA, Rasmussen SG, Thian FS, Kobilka TS, Choi HJ, Kuhn P, Weis WI, Kobilka BK, Stevens RC. High-resolution crystal structure of an engineered human beta2-adrenergic G protein-coupled receptor. Science 2007;318:1258. [PubMed: 17962520]

52. Markley JL, Ulrich EL, Westler WM, Volkman BF. Macromolecular structure determination by NMR spectroscopy. Methods Biochem Anal 2003;44:89. [PubMed: 12647383]

53. Veldkamp CT, Peterson FC, Hayes PL, Mattmiller JE, Haugner JC 3rd, de la Cruz N, Volkman BF. On-column refolding of recombinant chemokines for NMR studies and biological assays. Protein Expr Purif 2007;52:202. [PubMed: 17071104]

54. This work was supported by NIH grant R01 AI063325 (to BFV) and a Northwestern Mutual Fellowship from the MCW cancer center (to FCP). CTV was supported by a SpinOdyssey Postdoctoral Fellowship from the American Cancer Society, New England Division. The authors thank Paulette Hayes for assistance in SDF-1 protein production. Atomic coordinates, chemical shifts and structural constraints for each structural ensemble were deposited in the Protein Data Bank (PDB) and BioMagResBank: $SDF1_2$ (PDB 2K01; BMRB 15633), $SDF1_2$:p38 (PDB 2K04; BMRB 15636), $SDF1_2$:p38-sY1 (PDB 2K03; BMRB 15635), and $SDF1_2$:p38-sY3 (PDB 2K05; BMRB 15637).

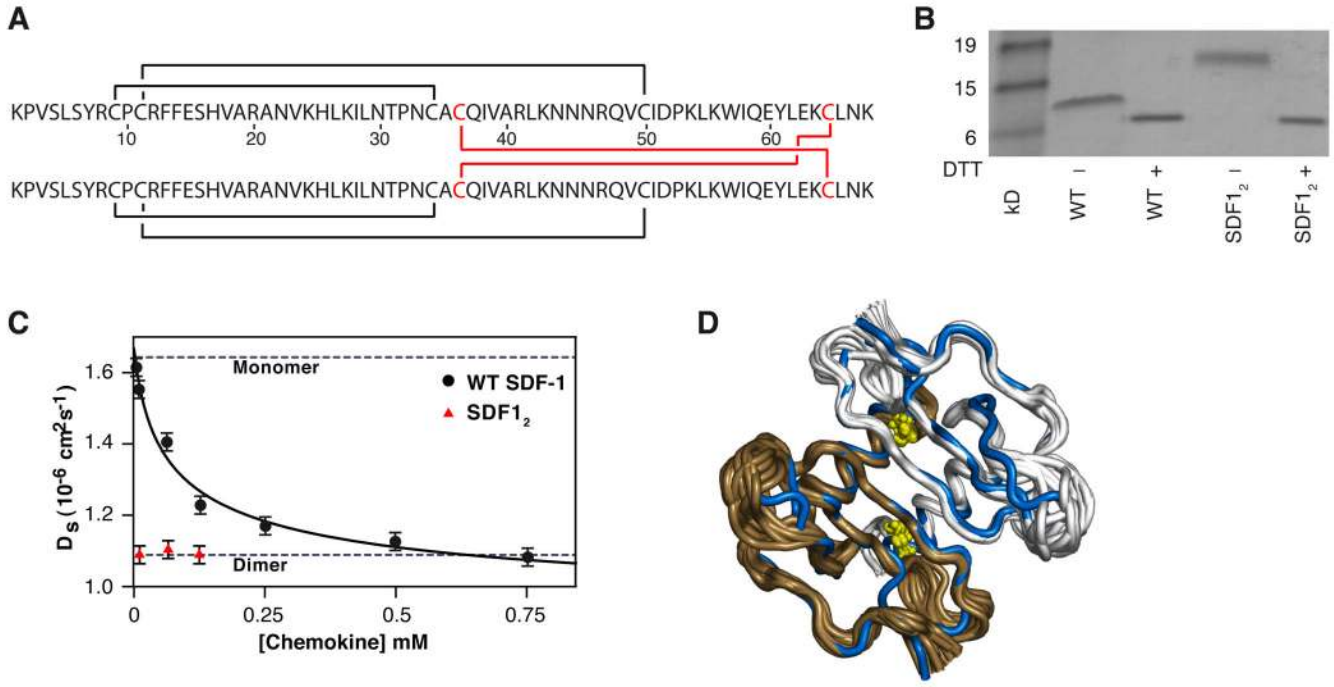

Fig. 1.

The NMR structure of disulfide-locked $SDF1_2$. (**A**) The amino acid sequence of $SDF1_2$ with the conserved intramolecular disulfide bonds (black lines) and the engineered intermolecular disulfide bonds (red lines) illustrated. (**B**) SDS-PAGE of SDF-1 and $SDF1_2$ treated with or without dithiothreitol (DTT). SDF-1 and $SDF1_2$ migrate near the monomeric molecular weight of 8 kD when treated with DTT. In contrast, whereas $SDF1_2$ migrates as a dimer, SDF-1 migrates as a monomer in the absence of DTT. (**C**) Translational diffusion measurements of $SDF1_2$ indicate that $SDF1_2$ is dimeric. Diffusion coefficients (Ds) of wild-type SDF-1 (black circles) in 20 mM sodium phosphate at pH 7.4 plotted against chemokine concentration (22). Nonlinear fitting of the Ds values of SDF-1 indicates a dimer dissociation Kd of 120 μM with a pure monomer Ds value of ~ 1.6 ($\times 10^{-6}$ cm^2s^{-1}) and a dimer value of ~1.0 ($\times 10^{-6}$ cm^2s^{-1}) [data from Veldkamp *et al.* (22)]. Ds values for 10, 50, and 150 μM $SDF1_2$ (red triangles) range from 1.08–1.09 ($\times 10^{-6}$ cm^2s^{-1}) consistent with those expected for SDF-1 in the dimeric state (data from this study). (**D**) Ensemble of 20 NMR solution structures of $SDF1_2$ (gray and tan) superimposed on the crystal structure of dimeric wild-type SDF-1 (blue, PDB ID 2J7Z) with an α-carbon RMSD of 1.2 Å for residues 9–66. Intermolecular Cys^{36}-Cys^{65} disulfide bonds are shown in yellow. Flexible N-terminal residues of SDF-1 (1–8) are omitted for clarity. Refinement statistics for the $SDF1_2$ structure ensemble are given in table S1.

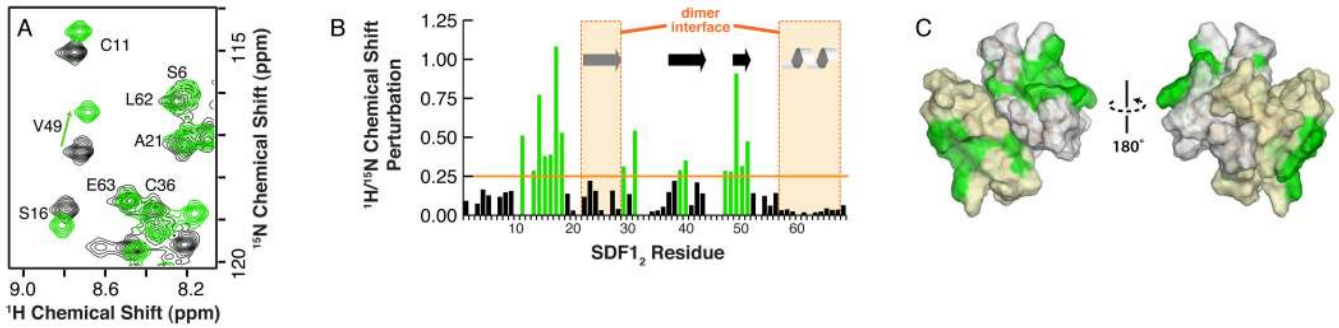

Fig. 2.

The N-terminus of CXCR4 binds to SDF1$_2$. (**A**) ^{15}N-^{1}H HSQC spectra of 25 μM [U-^{15}N]-SDF1$_2$ alone (black contours) and after the addition of 100 μM p38 peptide (green contours). (**B**) Combined ^{15}N-^{1}H chemical shift perturbations plotted against SDF1$_2$ residue number. Secondary structure elements are indicated and regions involved in the dimer interface are highlighted in orange. Missing values correspond to proline residues (sequence positions 2, 10,32, and 53) or amino acid residues not observed in the ^{15}N-^{1}H HSQC spectra. (**C**) Chemical shift mapping on the SDF1$_2$ structure. Green surface highlighting corresponds to shift perturbations > 0.25 in (**B**).

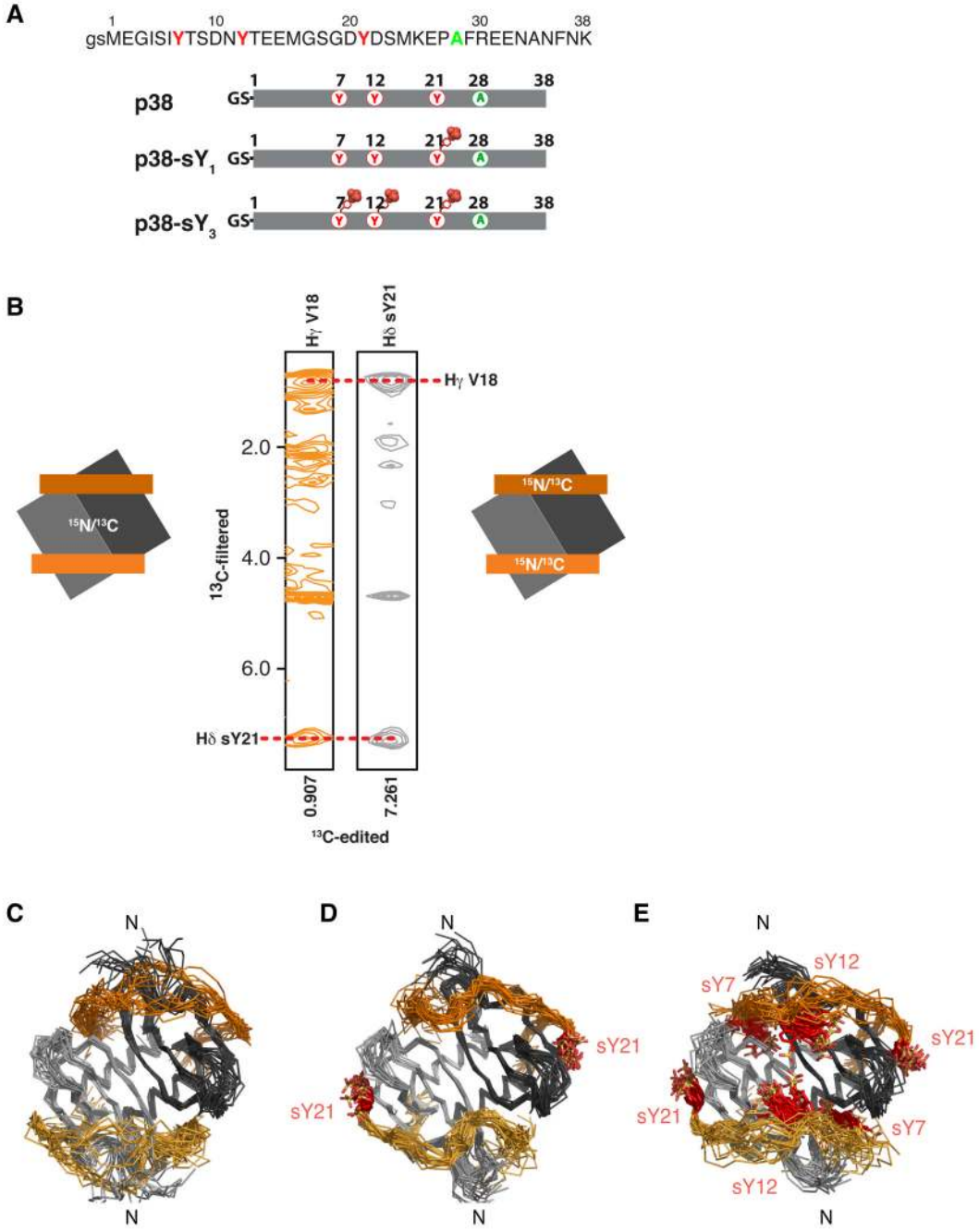

Fig. 3.

Structures of $SDF1_2$ dimers bound to the N-terminal domain of CXCR4. (**A**) N-terminal peptides corresponding to the first 38 amino acids of CXCR4 are illustrated. The sequence for p38 is identical to that of CXCR4 except for a Gly-Ser dipeptide on the N-terminus, which results from a cloning artifact, and a $Cys^{28} \rightarrow Ala^{28}$ mutation to prevent oxidative peptide dimer formation. The sulfated peptides are identical to p38 except for the inclusion of sulfotyrosine at position 21 for p38-sY_1 and at 7, 12, and 21 for p38-sY_3. (**B**) Representative intermolecular NOEs for the $SDF1_2$:p38-sY_1 complex. Strips from 3D F1-^{13}C-flitered/F3-^{13}C-edited NOESY-HSQC spectra acquired from a complex containing [U-^{15}N,^{13}C]-$SDF1_2$ and unlabeled p38-sY_1 (left) and a complex containing [U-^{15}N,^{13}C]-p38-sY_1 and

unlabeled $SDF1_2$ (right) contain equivalent NOEs between the methyl group of Val^{18} of $SDF1_2$ and $sTyr^{21}$ $^1H^{\delta}$ of p38-sY_1. Ensembles of the 20 lowest energy conformers for the $SDF1_2$:p38 (**C**), $SDF1_2$:p38-sY_1 (**D**), and $SDF1_2$:p38-sY_3 (**E**) complexes. $SDF1_2$ is shown in gray and the CXCR4 N-termini are orange. Sulfotyrosine residues in N-termini of CXCR4 are shown in red.

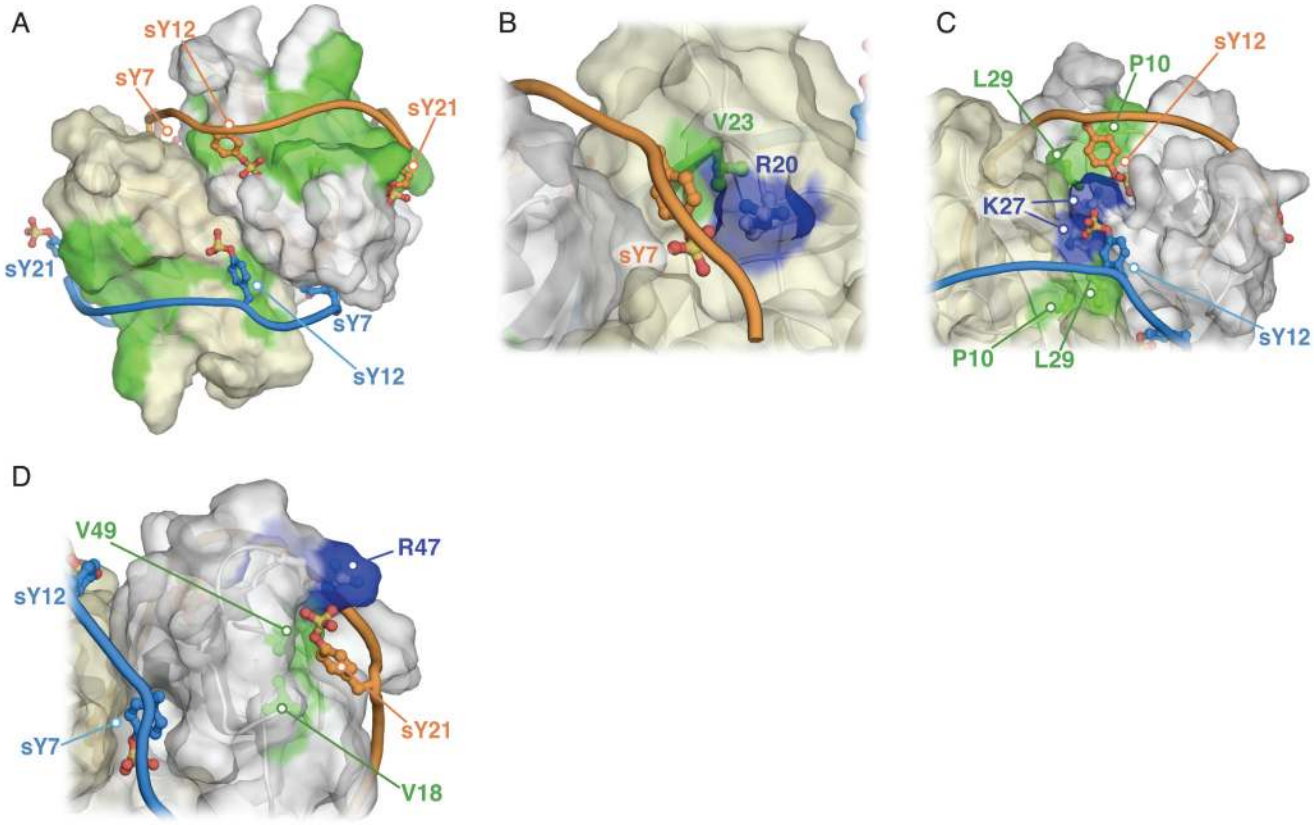

Fig. 4.

Recognition of sulfotyrosines by $SDF1_2$. (**A**) NMR structure of $SDF1_2$ bound to p38-sY_3. Individual subunits of the symmetric $SDF1_2$ dimer are shown in tan and white with symmetry-related p38-sY_3 peptides in blue and orange. Chemical shift perturbations greater than 0.25 ppm (Fig. 2C) are highlighted in green on the surface of $SDF1_2$. Flexible regions of $SDF1_2$ (residues 1–8) and p38-sY_3 (residues 29–38) are omitted for clarity. Sulfotyrosine side chains are shown in a ball-and-stick representation. In panels **B–D**, basic residues in $SDF1_2$ that pair with CXCR4 sulfotyrosines are shown in blue and $SDF1_2$ residues with NOEs to the sulfotyrosines are shown in green. (**B**) The $sTyr^7$ residue of CXCR4 binds to $SDF1_2$ near Arg^{20} and makes NOE contacts with Val^{23}. (**C**) The $sTyr^{12}$ residue of CXCR4 occupies a cleft bounded by residues Lys^{27}, Pro^{10}, and Leu^{29} of $SDF1_2$. (**D**) The $sTyr^{21}$ residue of CXCR4 pairs with Arg^{47} of $SDF1_2$ and makes NOE contacts with Val^{18} and Val^{49}.

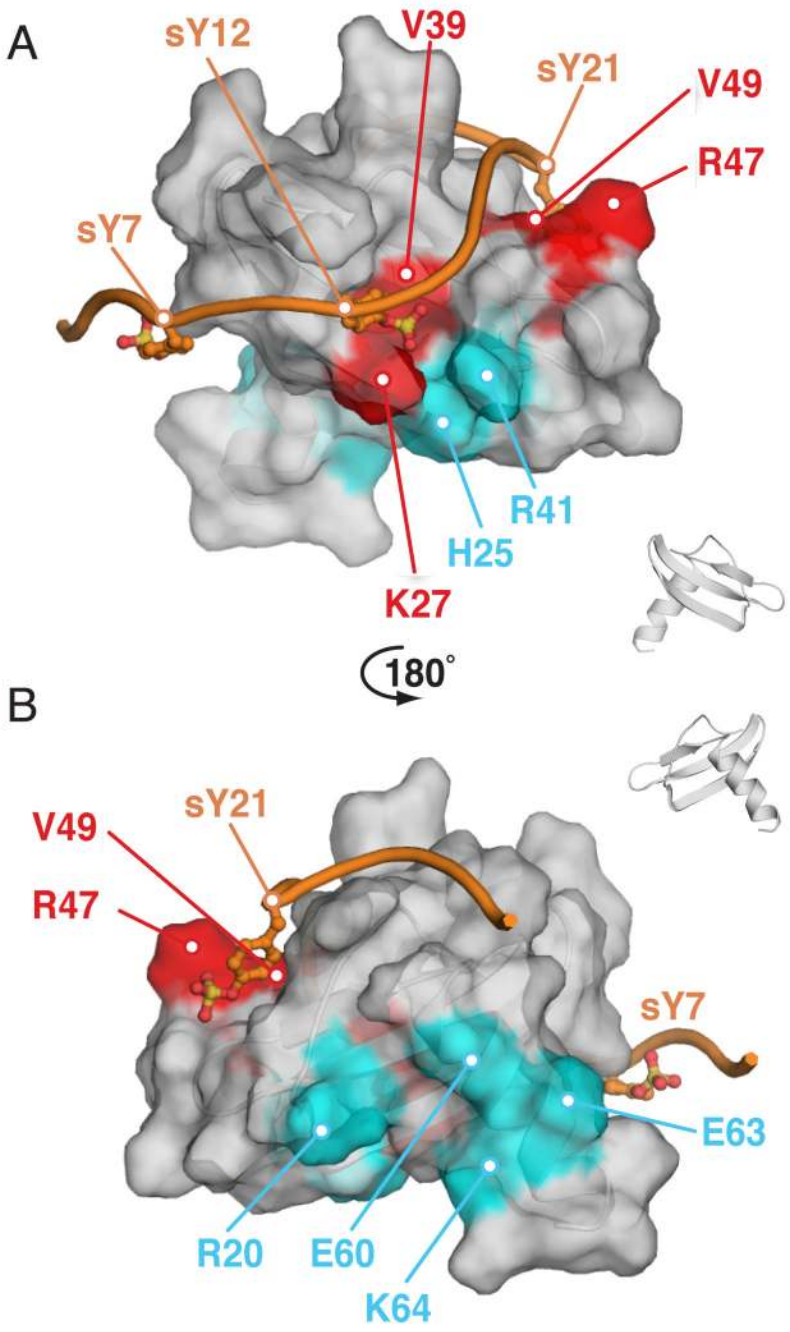

Fig. 5.

Amino acid substitutions in native SDF-1 corroborate the CXCR4 N-terminal binding site. One subunit of the $SDF1_2$ dimer and one p38-sY3 molecule from the $SDF1_2$:p38-sY_3 complex solved by NMR represent a model for the equivalent 1:1 complex. Front (**A**) and back (**B**) views of the SDF-1 surface are highlighted to indicate the location and functional impact of amino acid substitutions in the wild-type SDF-1 sequence. Substitutions at the $sTyr^{12}$- and $sTyr^{21}$-binding sites (red) showed increased EC_{50} values for Ca^{2+} mobilization, whereas substitutions away from the CXCR4-binding site (cyan) showed no change in their EC_{50} values. A binding site for $sTyr^7$ is not defined in this model because $sTyr^7$ binds to the opposing SDF-1 subunit in the $SDF1_2$:p38-sY3 structure.

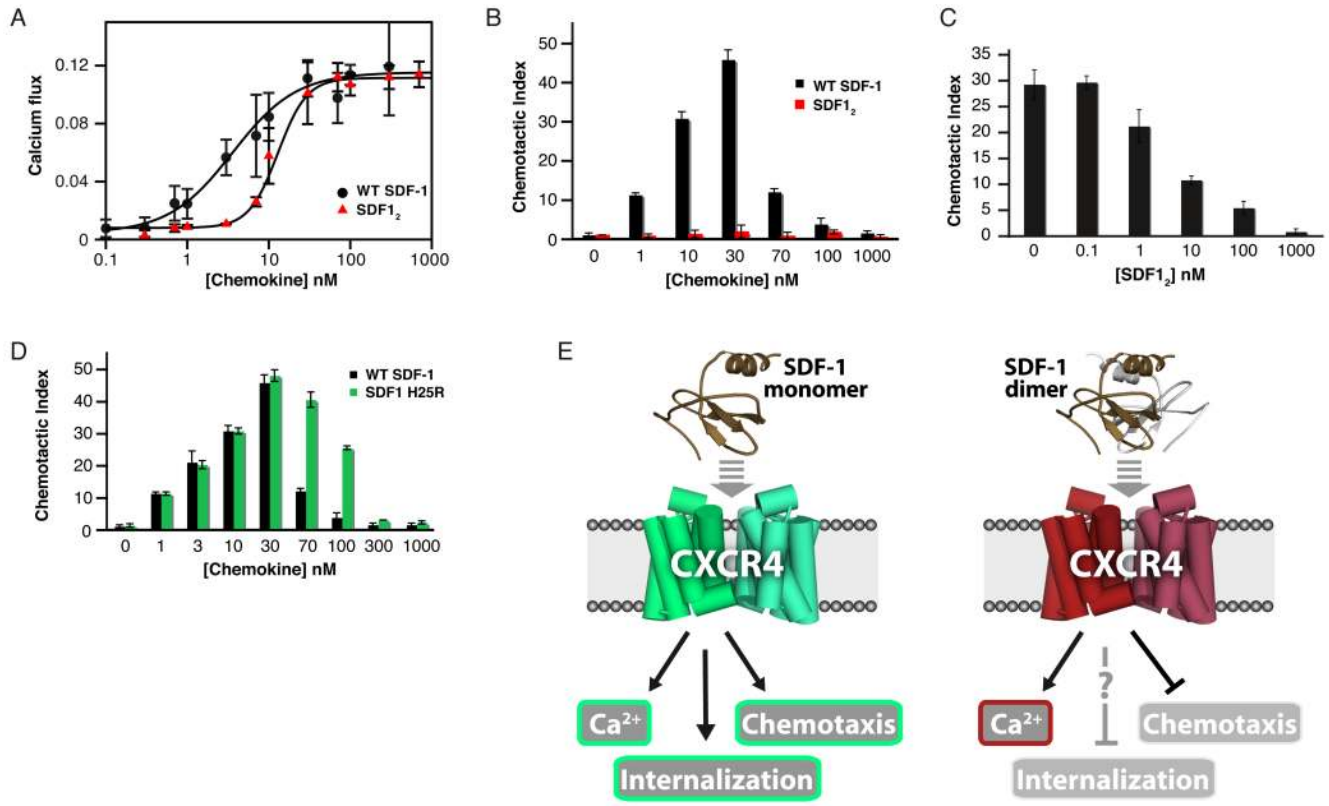

Fig. 6.

Dimeric SDF1$_2$ induces CXCR4-mediated Ca^{2+} mobilization but inhibits chemotaxis to wild-type SDF-1. (**A**) Ca^{2+} mobilization in THP-1 cells loaded with Fluo-3 indicates robust dose-dependant activation of CXCR4 by wild-type SDF-1 (●, EC_{50} = 3.6 nM) and SDF1$_2$ (▲, EC_{50} = 12.9 nM) (Data from Veldkamp *et al*. (53) and this study, respectively). (**B**) Wild-type SDF-1 induces the chemotaxis of THP-1 cells in a biphasic, concentration-dependent manner with a maximal migratory response at ~30 nM SDF-1. In contrast, SDF1$_2$ does not induce chemotaxis of THP-1 cells at any concentration from 1–1,000 nM. (**C**) Chemotaxis of THP-1 cells induced by 10 nM wild-type SDF-1 is inhibited by SDF1$_2$ (IC_{50} ~ 4 nM). (**D**) Wild-type SDF-1 and the dimerization-impaired $His^{25} \rightarrow Arg^{25}$ variant [SDF1(H25R)] induce chemotaxis of THP-1 cells equally well at low concentrations (0.1–10 nM). SDF1(H25R) remains monomeric at higher concentrations than does wild-type SDF-1 and induces chemotaxis over a broader range of concentrations. (**E**) Monomeric SDF-1 generates the full range of cellular responses to CXCR4 activation, whereas dimeric SDF1 is a partial agonist of CXCR4 that fails to induce chemotaxis. Loss of migration could be a consequence of aberrant CXCR4 trafficking.

Table 1

CXCR4 activation by SDF-1 mutants[a]

	EC_{50} (nM)[b]	Folded[c]	Fold Increase	p38 contact
SDF-1	3.6 ± 1.4	+		
$Arg^{20}Ala$	4.3 ± 0.6	+	1.2	+
$Val^{23}Ala$	NA	−	NA	+
$His^{25}Arg$	5.1 ± 0.9	+	1.4	−
$Lys^{27}Ala$	10.1 ± 2.9	+	2.8	+
$Lys^{27}Glu$	16.8 ± 1.1	+	4.7	+
$Val^{39}Ala$	27.1 ± 0.2	+	7.5	+
$Arg^{41}Ala$	4.3 ± 0.9	+	1.2	−
$Arg^{47}Ala$	14.1 ± 0.6	+	3.9	+
$Arg^{47}Glu$	654 ± 93	+	181.7	+
$Val^{49}Ala$	8.6 ± 2.4	+	2.4	+
$Glu^{60}Ala$	4.1 ± 0.1	+	1.1	−
$Glu^{63}Ala$	3.7 ± 0.8	+	1.0	−
$Lys^{64}Ala$	5.0 ± 1.1	+	1.4	−

[a] The current two-step, two-state model for CXCR4 activation implicates the SDF-1:p38 interaction in binding affinity and receptor specificity, but not in CXCR4 activation (12,26). A peptide consisting of SDF-1 residues 1–8 fully activates CXCR4 at micromolar concentrations (49), and because each SDF-1 variant retained the native N-terminus, the EC_{50} value in the Ca^{2+} mobilization assay should reflect its apparent affinity for CXCR4. Consequently, an amino acid substitution that alters the EC_{50} for Ca^{2+} mobilization relative to that of wild-type SDF-1 has necessarily disrupted an interaction between the chemokine and the N-terminus or extracellular loops of CXCR4.

[b] Values are reported as mean ± the standard deviation for two or more replicate measurements.

[c] The $^{1}H–^{15}N$ HSQC spectrum displays chemical shifts similar to wild-type SDF-1 except for residues adjacent to the site of mutation.